Partial oxidation of ethanol to hydrogen over Ni–Fe catalysts

Weiping Wang, Zhifei Wang, Yan Ding, Jinyu Xi, and Gongxuan Lu *

State Key Laboratory for Oxo Synthesis and Selective Oxidation, Lanzhou Institute of Chemical Physics, Chinese Academy of Sciences, Lanzhou 730000, China

Received 9 August 2001; accepted 9 January 2002

Catalytic generation of hydrogen by partial oxidation of ethanol over a series of Ni–Fe catalysts has been studied. The catalytic performances have been investigated under various O_2 and C_2H_5OH molar ratios at 473–573 K. These Ni–Fe catalysts showed high activities for the partial oxidation of ethanol to hydrogen. The rate of hydrogen generation increased with the increase of temperature. Among the different Ni–Fe catalysts, $Ni_{50}Fe_{50}$ had the best activity. The conversion of ethanol reaches 86.91% and selectivity to hydrogen reaches 46.23% at optimum reaction conditions, *i.e.*, $O_2/C_2H_5OH = 1.5$, $T = 573$ K. XRD patterns of the catalysts showed that their main components are spinal-type magnetite and $FeNi_3$ alloy. XPS results indicated that the bulk of catalyst is mainly $FeNi_3$ alloy and the surface is mainly magnetite. The possible mechanism has been discussed.

KEY WORDS: ethanol; partial oxidation; Ni–Fe catalyst; hydrogen.

1. Introduction

Being a clean burning and, potentially, a highly efficient energy carrier, hydrogen is being used more and more widely and will become a major energy source in the future. With the development of hydrogen fuel cell technology, the need for hydrogen as the energy resource for fuel cells becomes more urgent. However, the major impediment to the extensive use of hydrogen is the difficulty of its storage and distribution. The key problems for large-scale use of hydrogen are producing and storing hydrogen safely. One alternative solution to these problems is on-board hydrogen generation from a suitable high-energy-density liquid fuel. Among various liquid fuels, methanol and ethanol are considered as the potential resources because of their low cost, easy storage and transportation and high energy content.

Great attention has been paid to the study of methanol-to-hydrogen conversion and much improvement has been made [1–6]. From the view of renewable energy, ethanol can be produced from the biomass and will not give off net carbon dioxide to the environment. Furthermore, hydrogen produced by one mole of ethanol is 1.5 times as much as that of methanol. As an energy resource of fuel cells, ethanol is more promising. Nevertheless, the catalytic generation of hydrogen from ethanol has not been fully investigated [7–15]. Nowadays, the study of ethanol-to-hydrogen conversion mainly concentrates on theoretical thermodynamic analysis and ethanol steam reforming. Some active catalysts can operate at relatively high temperature; for example, Ni/La_2O_3 catalyst is active for ethanol steam reforming at 973–1073 K [14]. However, an active catalyst at relatively low temperature is more attractive from the practical point of view because this process can be operated with waste heat from the engine at 573–673 K. Partial oxidation of ethanol to hydrogen, especially, is an exothermic reaction and is now applicable to fuel cell systems because of its easy handling, low cost and no requirement of additional heating apparatus. Ethanol partial oxidation does not need many facilities, since only ethanol and air are consumed, and it can be operated under self-thermal-balanced conditions. The reaction equations of ethanol partial oxidation to hydrogen are:

$$C_2H_5OH + \tfrac{1}{2}O_2 \longrightarrow 2CO + 3H_2 \qquad \Delta H^{\circ}_{298} = 14.1\ \text{kJ/mol}$$

$$C_2H_5OH + \tfrac{3}{2}O_2 \longrightarrow 2CO_2 + 3H_2 \qquad \Delta H^{\circ}_{298} = -554.0\ \text{kJ/mol}$$

Up to now, the study of partial oxidation of ethanol to hydrogen has seldom been carried out.

In this paper we used a co-precipitation technique to prepare the Ni–Fe catalysts. Catalytic activities for partial oxidation of ethanol were investigated under different conditions. We found that Ni–Fe catalysts are very active for ethanol partial oxidation to hydrogen at a relatively low temperature (573 K). The catalysts were characterized by powder X-ray diffraction (XRD) and X-ray photoelectron spectroscopy (XPS).

2. Experimental

2.1. Preparation of catalysts

Ni–Fe catalysts with different weight ratios of metallic Ni and Fe were prepared by co-precipitation.

* To whom correspondence should be addressed.

1011-372X/02/0700-0063/0

An aqueous solution of Na_2CO_3 was added drop-wise to an aqueous solution of $Ni(NO_3)_2$ and $Fe(NO_3)_3$ with vigorous stirring at room temperature. The resulting precipitate was filtered, washed thoroughly with distilled water and dried in air at 383 K for 10 h. The co-precipitated catalyst precursors were then calcined in air at 673 K for 3 h and crushed to 40–60 mesh.

2.2. Catalytic tests

The calcined catalysts were reduced *in situ* by 10% H_2 diluted with N_2 stream (flow rate 30 ml/min) at 573 K for 3 h before test. Catalytic tests were performed in a fixed-bed continuous flow quartz reactor (4 mm i.d.). Typically, 200 mg of catalyst was used for each run. Ethanol was supplied by saturating N_2 and oxygen carriers in a set of jacketed saturators maintained in an external heating bath which could ensure that the ethanol flow rate was 5 ml/min; the total flow rates were kept at 35 ml/min. After reaction for 20 min, the products were analyzed by two on-line gas chromatographs equipped, respectively, with a 13× molecular sieve column and a Porapak-Q column with two thermal-conductivity detectors (TCD). Hydrocarbons as well as oxygenated products were separated by a Porapak-T column and analyzed by a flame ionization detector (FID). The catalysts were cooled to room temperature in a nitrogen stream to prevent oxidation.

2.3. Characterization

The BET surface areas of the calcined samples, before the reaction, were estimated by nitrogen adsorption experiments on an ST-03 (China). The powder XRD patterns of Ni–Fe catalysts were recorded on a Rigaku D/MAX-RB X-ray diffractometer with Cu K_α radiation and Ni filter to identify the species in the catalysts. XRD measurements were conducted in a scanning angle (2θ) range of 20–70° at a scanning speed of 4 deg/min.

X-ray photoelectron spectra (XPS) were measured on a VG-ESCALAB 210 with Mg K_α radiation ($h\nu = 1253.6$ eV). If necessary, the sample was ion-sputtered by Ar ions for 0, 30, 60 or 90 min at 3 kV and 80 mA before measurement. The binding energies are calibrated by the C_{1S} binding energy of 250.0 eV.

3. Results and discussion

3.1. Catalytic activity for partial oxidation of ethanol

Partial oxidation of ethanol reaction was conducted under normal pressure at 473–573 K with the O_2/C_2H_5OH mole ratio varied from 0 to 2.0. The hydrogen selectivity is defined as $(\frac{1}{3}\text{mol}\,H_{2\,\text{produced}})/(1\,\text{mol}\text{-}C_2H_5OH_{\text{fed}})$ and the definitions of selectivities of carbon dioxide and carbon monoxide are similar to H_2.

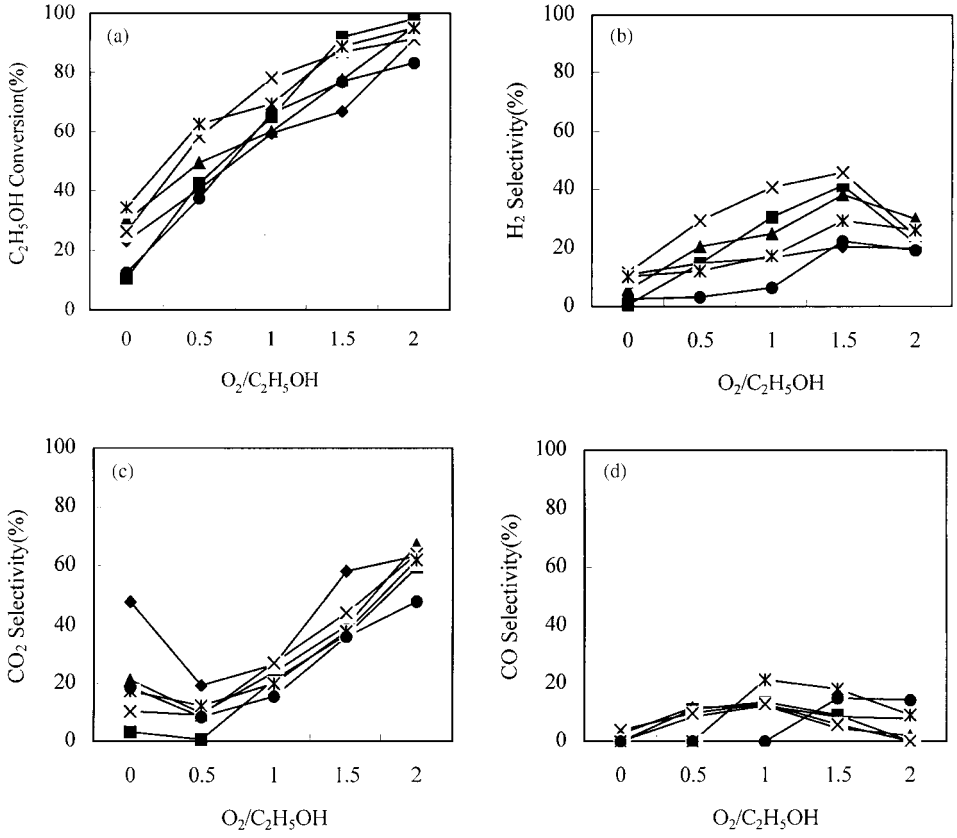

Figure 1. Effect of O_2/C_2H_5OH ratio on ethanol conversion and selectivity over different Ni–Fe catalysts. (a) Ethanol conversion; (b) H_2 selectivity; (c) CO_2 selectivity; (d) CO selectivity. ◆, $Ni_{90}Fe_{10}$; ■, $Ni_{70}Fe_{30}$; ▲, $Ni_{60}Fe_{40}$; ×, $Ni_{50}Fe_{50}$; ✳, $Ni_{30}Fe_{70}$; ●, $Ni_{10}Fe_{90}$.

Figure 1 shows the catalytic performance at 573 K over different Ni–Fe catalysts. The conversion of ethanol increases gradually with the increase of O_2/C_2H_5OH molar ratio over various Ni–Fe catalysts (see figure 1). For the $Ni_{50}Fe_{50}$ catalyst, the ethanol conversion is close to 30% in the absence of O_2 (corresponding to the ethanol decomposition reaction). When the O_2/C_2H_5OH molar ratio reaches the stoichiometric ratio (1.5), the ethanol conversion is nearly 90%, which indicated that the addition of oxygen could enhance the partial oxidation of ethanol to hydrogen. Hydrogen selectivity increases at first with the increase of the O_2/C_2H_5OH ratio and reaches a maximum value at an O_2/C_2H_5OH ratio of 1.5 (see figure 1), and then decreases obviously. Typically, the H_2 selectivity is 44.03% at an ethanol conversion of 86.91% when the O_2/C_2H_5OH ratio is 1.5 for $Ni_{50}Fe_{50}$ catalyst. However, the H_2 selectivities over $Ni_{90}Fe_{10}$ and $Ni_{10}Fe_{90}$ catalysts are only 20.59% and 22.03% under the same conditions respectively. When the O_2/C_2H_5OH ratio increases to 2.0, H_2 selectivity decreases significantly because excess O_2 results in H_2 oxidation to H_2O. In addition, selectivity to hydrogen of $Ni_{50}Fe_{50}$ catalyst is higher than that of other samples at the O_2/C_2H_5OH ratios from 0.5 to 1.5.

We detected trace amount of the by-product CH_4 only at 573 K. The by-product CO_2 is formed both in the presence and in the absence of oxygen. For the $Ni_{50}Fe_{50}$ catalyst, we found the CO_2 selectivity was 10.24% in the absence of O_2. Addition of O_2 results in the decrease of CO_2 selectivity at first, and is followed by the increase for all Ni–Fe catalysts. The minimum value of CO_2 selectivity appears at the O_2/C_2H_5OH ratio of 0.5 (see figure 1). CO selectivity initially raises and then decreases with the increase of the O_2/C_2H_5OH ratio, but remains at quite low values in all cases. The maximum CO_2 selectivity occurs at the O_2/C_2H_5OH ratio of 1.0 (see figure 1) except for the $Ni_{10}Fe_{90}$ catalyst. For example, the CO selectivity of the $Ni_{50}Fe_{50}$ catalyst is less than 5.84% at the O_2/C_2H_5OH ratio of 1.5 and becomes zero at the O_2/C_2H_5OH ratio of 2.0.

Reaction temperature markedly affects H_2 selectivity (see figure 2) and ethanol conversion. The ethanol conversion increases with reaction temperature. For example, the conversion of ethanol reaches 70% over the $Ni_{50}Fe_{50}$ catalyst at 473 K, O_2/C_2H_5OH ratio of 1.5, but the conversion of ethanol reaches 86.91% at 573 K with the same O_2/C_2H_5OH ratio. Within the temperature range 473–573 K, the selectivity to H_2 increases with the increase of reaction temperature and reaches a maximum value at 573 K. It is interesting that $Ni_{60}Fe_{40}$ catalyst shows high catalytic activity at rather low temperature (498–523 K). For instance, the selectivity to hydrogen has already reached 18.03% at 523 K with an O_2/C_2H_5OH ratio of 1.5, which corresponds to an ethanol conversion of 49.1%. It is surprising to find that hydrogen selectivities are almost zero over $Ni_{70}Fe_{30}$, $Ni_{50}Fe_{50}$ and $Ni_{10}Fe_{90}$ catalysts at 498–523 K, but they exceed 20.17% when the reaction temperature increases to 548 K. Increasing the reaction temperature results in the significant increase of selectivity to hydrogen and conversion of ethanol. Selectivity to hydrogen is clearly higher over $Ni_{50}Fe_{50}$ than that of other catalysts at relatively high temperature (548–573 K) and reaches a maximum value of 46.23%, while the conversion of ethanol is 86.91% at 573 K. From a practical point of view, low temperature activity may be important since waste heat of the engine (around 573 K) can be used in the facility.

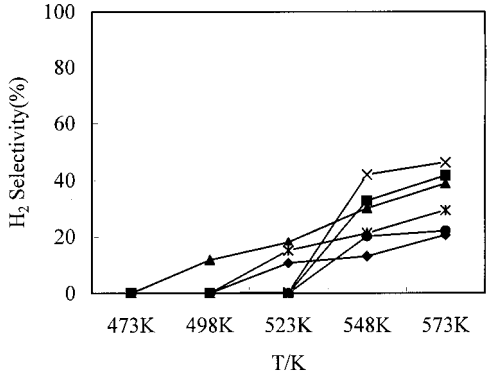

Figure 2. Effect of temperature on hydrogen selectivity over different Ni–Fe catalysts at $O_2/C_2H_5OH = 1.5$. ◆, $Ni_{90}Fe_{10}$; ■, $Ni_{70}Fe_{30}$; ▲, $Ni_{60}Fe_{40}$; ×, $Ni_{50}Fe_{50}$; ✳, $Ni_{30}Fe_{70}$; ●, $Ni_{10}Fe_{90}$.

Oxygen conversion is 100% in our experimental conditions. Oxygen is consumed completely during partial oxidation of ethanol reaction at O_2/C_2H_5OH ratios from 0.5 to 2.0. Further increase of the O_2/C_2H_5OH ratio causes the decrease of H_2 selectivity and the increase of selectivities to CO_2 and H_2O. Among all Ni–Fe catalysts, $Ni_{50}Fe_{50}$ shows fairly high activity and selectivity; the optimum reaction conditions are 573 K and $O_2/C_2H_5OH = 1.5$.

3.2. Activity with time-on-stream—stability test

The stability of the $Ni_{50}Fe_{50}$ catalyst has been examined at 573 K and the results are shown in figure 3, in which the alterations of activity and selectivity to hydrogen are plotted as functions of time on stream. Under the experimental conditions employed (see figure 3), there is a small increase of ethanol conversion (from 90.42 to 96.86%) during the first 1–10 h on stream, while hydrogen selectivity drops from 51.67 to 47.12%. During the next 15 h on stream, ethanol conversion and hydrogen selectivity ultimately maintain constancy. However, ethanol conversion increases to 100% at 40 h, while hydrogen selectivity obviously decreases after reaction for 25 h, and drops to 27.31% at 40 h, which was probably due to the carbon formation. Work to increase the stability of $Ni_{50}Fe_{50}$ catalyst is still in progress.

3.3. BET surface area

The BET surface area of catalysts was determined by the nitrogen adsorption method (see table 1). $Ni_{70}Fe_{30}$

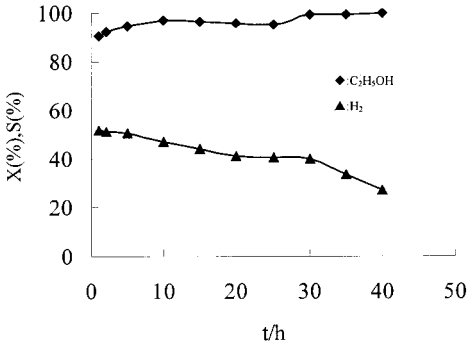

Figure 3. Conversion of ethanol and selectivity to hydrogen as a function of time-on-stream over $Ni_{50}Fe_{50}$ catalyst. Experimental conditions: catalyst 200 mg; $O_2/C_2H_5OH = 1.5$; $T = 573$ K; $P = 1$ atm.

catalyst has the highest BET surface area, while $Ni_{60}Fe_{40}$ has the lowest. As compared with the data of activity, we concluded that BET surface area of samples does not have a direct effect on activity.

3.4. XRD study

Figure 4 shows the powder XRD patterns of Ni–Fe catalysts after ethanol partial oxidation at 573 K and $O_2/C_2H_5OH = 2.0$. It can be seen that different catalysts exhibited similar diffraction patterns. The Fe and Ni species in these catalysts can be identified as spinel-structured $(Ni,Fe)Fe_2O_4$ and $FeNi_3$ alloy, respectively; no Fe metallic or FeO or other phases are found. In the used catalysts, the sharp peaks attributed to $FeNi_3$ alloy are observed at $2\theta = 44.2^\circ$ and 51.6°, as well as the typical peaks of $(Ni,Fe)Fe_2O_4$ with spinel structures. The intensities of $FeNi_3$ alloy diffraction peaks decrease with the decrease of Ni content in the catalysts. For example, significant decreases of intensities of $FeNi_3$ alloy diffraction peaks occur when Ni content is reduced from 70 to 60%. However, the diffraction patterns of $(Ni,Fe)Fe_2O_4$ remain almost unchanged when the Ni content is reduced. The possible reason may be the high stability of the $(Ni,Fe)Fe_2O_4$ structure. The peaks of fresh $Ni_{50}Fe_{50}$ catalyst are broad and weak—as shown in figure 5—while these peaks become sharp after reaction. The reason may be that the $(Ni,Fe)Fe_2O_4$ crystals re-construct during the reaction, which results in the growth of the crystal size of the catalyst. Since the selectivity to H_2 only reached 23.3% over pure NiO even at 573 K in blank runs, while pure Fe_2O_3 was hardly active for partial oxidation of ethanol to hydrogen, spinel-structured $(Ni,Fe)Fe_2O_4$ and $FeNi_3$ alloys are, probably, the active species for ethanol partial oxidation to hydrogen. An appropriate content of $(Ni,Fe)Fe_2O_4$ and $FeNi_3$ alloy in the catalyst results in a higher catalytic activity.

Table 1
BET surface area of catalysts

Catalyst	$Ni_{70}Fe_{30}$	$Ni_{60}Fe_{40}$	$Ni_{50}Fe_{50}$
S_{BET} (m^2/g)	126	92.7	104

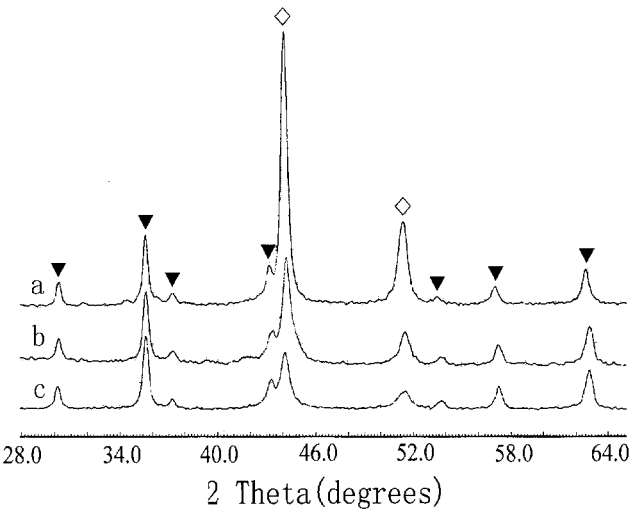

Figure 4. XRD patterns of the used Ni–Fe catalysts. (a) $Ni_{70}Fe_{30}$; (b) $Ni_{60}Fe_{40}$; (c) $Ni_{50}Fe_{50}$. ▼, $(Ni,Fe)Fe_2O_4$; ◇, $FeNi_3$.

3.5. XPS study

XPS was used to study the chemical state of surface species in the catalysts. Figure 6 shows the Ni XPS patterns of $Ni_{50}Fe_{50}$ and $Ni_{70}Fe_{30}$ catalysts after sputtering of argon ions for different times. Only oxidized Ni species and Fe species are observed before sputtering in these two catalysts. The binding energies of Ni $2p_{3/2}$ and Fe $2p_{3/2}$ for $Ni_{70}Fe_{30}$ catalyst are 856.08 eV and 711.36 eV, respectively. After a short sputtering time, the binding energy of Ni $2p_{3/2}$ changes to 853.47 eV, *i.e.*, has a shift about 2.61 eV to the low binding energy region, and the peak becomes much narrower and the satellite peaks disappear. These phenomena show that there is a large content of metallic Ni species in the bulk phase. Considering the XRD results, it is believed that the sample bulk phase is mostly alloy phase and the surface is the oxidized species. This result was further supported by the Fe XPS (see figure 7) study. One XPS peak with binding energy of 711.36 eV is observed for

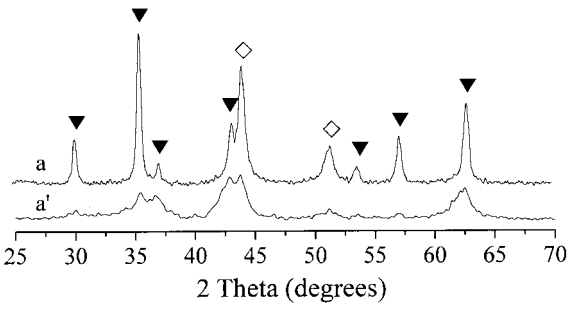

Figure 5. XRD patterns of the fresh and used $Ni_{50}Fe_{50}$ catalysts. (a) Used catalyst; (a′) fresh catalyst. ▼, $(Ni,Fe)Fe_2O_4$; ◇, $FeNi_3$.

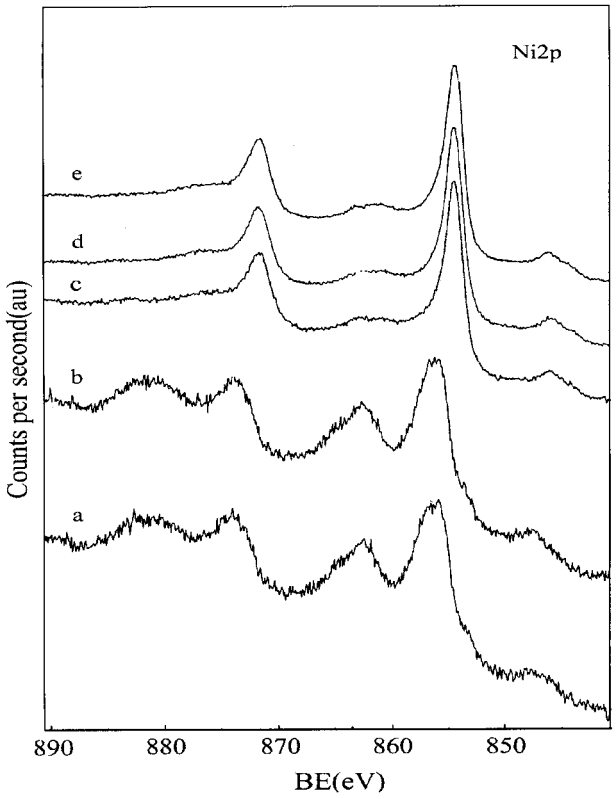

Figure 6. XPS patterns of Ni 2p for $Ni_{50}Fe_{50}$ and $Ni_{70}Fe_{30}$ catalysts. (a) $Ni_{50}Fe_{50}$; (b) $Ni_{70}Fe_{30}$; (c) $Ni_{70}Fe_{30}$ sputtering for 30 min; (d) $Ni_{70}Fe_{30}$ sputtering for 60 min; (e) $Ni_{70}Fe_{30}$ sputtering for 90 min.

the Fe $2p_{3/2}$ before sputtering, which is assigned to the oxidized ferrite on the surface of the sample. After sputtering, the pattern of Fe $2p_{3/2}$ broadened and split to dual peaks, at 707.86 eV and 710.53 eV, respectively. They are assigned to Fe $2p_{3/2}$ of metallic Fe and that of dispersed oxidized Fe phase. The surface atomic ratios of both species after sputtering for 30 min and 90 min are 1.00 and 1.331 respectively, *i.e.*, the surface concentration of metallic Fe atoms increases with sputtering time. The binding energies of metallic Ni and Fe are higher than those of the standard XPS data. It can be suggested that there is an interaction between metallic Ni and Fe. Taking the XRD results into consideration, we believe that Ni and Fe form $FeNi_3$ alloy rather than exist as pure metal.

Table 2
Surface atomic ratios of M and Fe(III) 2p calculated from XPS (M = metallic Fe 2p, metallic Ni 2p, Ni(II)2p)

	Sputtering time			
	$Ni_{50}Fe_{50}$ for 0 min	$Ni_{70}Fe_{30}$ for 0 min	$Ni_{70}Fe_{30}$ for 30 min	$Ni_{70}Fe_{30}$ for 90 min
Metallic Fe 2p /Fe(III) 2p	0	0	1.00	1.331
Metallic Ni 2p/Fe(III) 2p	0	0	4.15	5.384
Ni(II) 2p/Fe(III) 2p	1.29	2.45	0	0

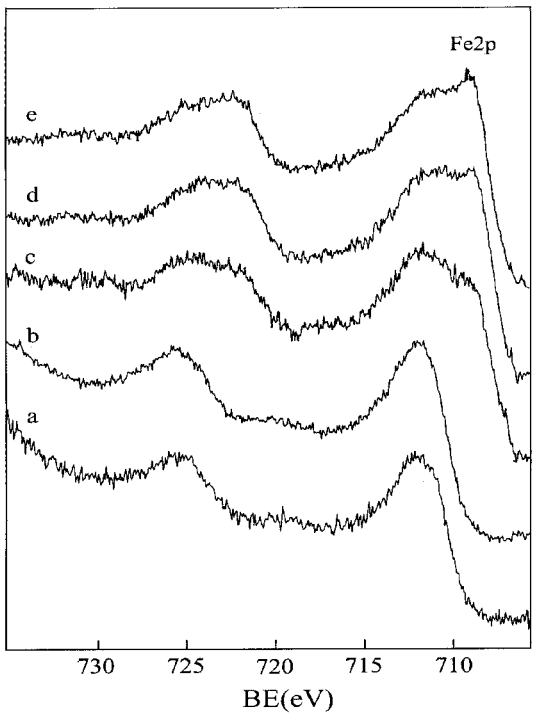

Figure 7. XPS patterns of Fe 2p for $Ni_{50}Fe_{50}$ and $Ni_{70}Fe_{30}$ catalysts. (a) $Ni_{50}Fe_{50}$; (b) $Ni_{70}Fe_{30}$; (c) $Ni_{70}Fe_{30}$ sputtering for 30 min; (d) $Ni_{70}Fe_{30}$ sputtering for 60 min; (e) $Ni_{70}Fe_{30}$ sputtering for 90 min.

In addition, from the XPS data we know that the sodium contents in $Ni_{50}Fe_{50}$ and $Ni_{70}Fe_{30}$ catalysts scarcely changed, even after the sputtering of $Ni_{70}Fe_{30}$ catalyst. So we concluded that sodium content does not have a remarkable effect on the catalytic performance of Ni–Fe catalysts.

4. Conclusions

The performances of different Ni–Fe catalysts have been investigated at 473–573 K, with the feed ratios of O_2/C_2H_5OH (molar) from 0 to 2.0. The experimental results indicate that Ni–Fe catalysts have a high catalytic activity to partial oxidation of ethanol to hydrogen. Catalytic activity increased with the increase of temperature. Among the catalysts, $Ni_{50}Fe_{50}$ has the best activity results. The selectivity to hydrogen of 50.66% and the ethanol conversion of 86.91% are obtained under the optimum reaction conditions: $T = 573$ K, $O_2/C_2H_5OH = 1.5$. The highest selectivity to H_2 is obtained at $O_2/C_2H_5OH = 1.0$, the low selectivity to CO is achieved at $O_2/C_2H_5OH = 2.0$ and the low selectivity to CO_2 is achieved at $O_2/C_2H_5OH = 0.5$ over $Ni_{50}Fe_{50}$ catalyst. XRD results of the fresh and used catalysts show that Ni–Fe catalysts are composed mainly of spinel-structural $(Ni,Fe)Fe_2O_4$ and $FeNi_3$ alloy. In addition, XPS results indicate that the surface of the sample mainly consists of oxidized species, while the bulk is mainly $FeNi_3$ alloy. Our present results

reveal that Ni–Fe catalysts exhibit high activity for partial oxidation of ethanol to hydrogen with high selectivity to hydrogen and conversion of ethanol. To our knowledge, our work is the first example of ethanol-to-hydrogen *via* partial oxidation at such a low temperature, 573 K (~300 °C).

Acknowledgments

The authors are grateful to the 973 project of China (G20000264).

References

[1] N. Takezawa, H. Kobayashi, A. Hirase and K. Takahashi, Appl. Catal. 4 (1982) 127.
[2] L. Alejo, R. Lago, M.A. Pena and J.L.G. Fierro, Appl. Catal. A 162 (1997) 281.
[3] M.L. Cubeiro and J.L.G. Fierro, J. Catal. 179 (1997) 150.
[4] S. Velu, K. Suzuki and T. Osaki, Catal. Lett. 62 (1999) 159.
[5] S. Velu, K. Suzuki, M.P. Kapoor, F. Ohashi and T. Osaki, Appl. Catal. A 213 (2001) 47.
[6] J. Agrell, K. Hasselbo and M. Boutonnet, Appl. Catal. A 211 (2001) 239.
[7] E.Y. Garcia and M.A. Laborde, Int. J. Hydrogen Energy 16 (1991) 307.
[8] K. Vasudeva, N. Mitra and P. Umasankar, Int. J. Hydrogen Energy 21 (1996) 13.
[9] I. Fishtik, A. Alexander and R. Datta, Int. J. Hydrogen Energy 25 (2000) 31.
[10] C.A. Luengo, G. Ciampi and M.O. Cencig, Int. J. Hydrogen Energy 17 (1992) 677.
[11] S. Cavallaro and S. Freni, Int. J. Hydrogen Energy 21 (1996) 465.
[12] F.J. Marino, E.G. Cerrella and S. Duhalde, Int. J. Hydrogen Energy 23 (1998) 1095.
[13] J. Lorca, P.R. Piscina, J. Sales and N. Homs, Chem. Commun. (2001) 641.
[14] A.N. Fatsikostas, D.I. Kondarides and X.E. Verykios, Chem. Commun. (2001) 851.
[15] J.Y. Xi, Z.F. Wang, W.P. Wang and G.X. Lu, J. Mol. Catal. (China) (in press).